X-rays from old open clusters: M 67 and NGC 188

Belloni, T.; Verbunt, F.; Mathieu, R.D.

Published in:
Astronomy & Astrophysics

Astron. Astrophys. 339, 431–439 (1998)

ASTRONOMY AND ASTROPHYSICS

X-rays from old open clusters: M 67 and NGC 188

T. Belloni[1], **F. Verbunt**[2], **and R.D. Mathieu**[3]

[1] Astronomical Institute "Anton Pannekoek", University of Amsterdam and Center for High-Energy Astrophysics, Kruislaan 403, 1098 SJ Amsterdam, The Netherlands
[2] Astronomical Institute, P.O.Box 80000, 3508 TA Utrecht, The Netherlands
[3] Department of Astronomy, University of Wisconsin, Madison, WI 53706, USA

Received 15 July 1998 / Accepted 17 August 1998

Abstract. We have observed the old open clusters M 67 and NGC 188 with the ROSAT PSPC. In M 67 we detect a variety of X-ray sources. The X-ray emission by a cataclysmic variable, a single hot white dwarf, two contact binaries, and some RS CVn systems is as expected. The X-ray emission by two binaries located below the subgiant branch in the Hertzsprung Russell diagram of the cluster, by a circular binary with a cool white dwarf, and by two eccentric binaries with $P_b \gtrsim 700\,\mathrm{d}$ is puzzling. Two members of NGC 188 are detected, including the FK Com type star D719. Another possible FK Com type star, probably not a member of NGC 188, is also detected.

Key words: stars: abundances – open clusters: individual: M 67; NGC 188 – X-rays: stars

1. Introduction

An observation of a stellar cluster is an observation of a population of stars of the same age. X-ray observations of open clusters with various ages can thus be used to learn how the X-ray emission of stars changes as they evolve. It is found in young clusters that stars with spectral types later than F emit X-rays due to rapid rotation. As these stars age, their rotation slows down, and their X-ray emission decreases (e.g. Caillault 1996, Randich et al. 1996 and references therein). An observation of M 67 with ROSAT discovered X-rays not only from the cataclysmic variable for which the observation was intended, but also from six other member stars (Belloni et al. 1993, hereafter BVS). Several of these other member stars are known to be binaries, and thus Belloni et al. suggested that their X-ray emission is due to rapid rotation caused by tidal interaction, i.e. that these X-ray sources are similar to the RS CVn binaries, which are well known X-ray emitters (e.g. Dempsey et al. 1993). In the strict definition, the rapidly rotating star in RS CVn binaries is a subgiant. If the Hertzsprung Russell diagram of a cluster shows a Hertzsprung gap, i.e. if the turnoff mass is higher than about 2.2 $M_\odot$, it is less likely to contain such RS CVn systems, as the (sub-)giants in these clusters live shorter. This has been confirmed with X-ray observations of such clusters as NGC 752 (Belloni & Verbunt 1996) and NGC 6940 (Belloni & Tagliaferri 1997). We use a less stringent definition of RS CVn binaries, which includes chromospherically active binaries consisting of two main-sequence stars, i.e. BY Draconis binaries.

In this paper we continue our study of the X-ray emission of old open clusters. We describe the results of a second, longer, X-ray observation of M 67, and of an X-ray observation of another old galactic cluster, NGC 188. We also reanalyse our first observation of M 67, and make use of new optical studies of the binaries in this cluster to determine the nature of the X-ray sources.

M 67 is an ideal target for ROSAT, due to its proximity at about 850 pc and the low interstellar absorption at $E(B-V) \simeq 0.03$ (Twarog & Anthony-Twarog 1989), which may be converted into a hydrogen column $N_\mathrm{H} \simeq 1.7 \times 10^{20}\mathrm{cm}^{-2}$ (Predehl & Schmitt 1995). (Note that these values differ from those used by BVS.) Its age is estimated to be about 4 Gyr (Dinescu et al. 1995). NGC 188 is at a larger distance of about 2 kpc and is reddened more at $E(B-V) = 0.09$ (von Hippel & Sarajedini 1998), or $N_\mathrm{H} \simeq 5.0 \times 10^{20}\mathrm{cm}^{-2}$. It is thought to be about 6 Gyr old (Dinescu et al. 1995).

2. Observations and data analysis

2.1. M 67

2.1.1. X-ray data

We observed M 67 with the ROSAT PSPC between April 25 and May 9 1993, for a total exposure of 15771 seconds; the center of the field of view was at 8h51m24.0s, 11°49′48.0″, the center of the cluster. Our previous PSPC observation, obtained between 15 and 19 November 1991, had a total exposure of 10515 seconds, and was centered at 8h50m24.0s, 11°49′12.0″, about 10′ offset from the center of the cluster (Belloni et al. 1993). The data were analyzed with the EXSAS package (Zimmermann et al. 1994). We also re-analyzed the previous pointing, both separately and merged with the new data. Since the PSPC point-spread function is not well known at large off-axis angles, we limited our analysis to the central 20′ of the instrument. We followed the standard EXSAS detection procedure (see e.g. BVS), whose final step consists of a Maximum Likelihood detection (Cruddace et al. 1988) in three separate bands: Total

Send offprint requests to: T. Belloni

(PHA channels 11-240, 0.1-2.4 keV), Soft (ch. 11-40, 0.1-0.4 keV) and Hard (ch. 41-240, 0.4-2.4 keV). We ran the detection procedure on the single observations, with a maximum likelihood threshold of acceptance of 13. This value is higher than the standard value of 10, but has been chosen on the basis of a visual inspection of the image, which also allowed us to discard obvious spurious detections. The detected sources in the three bands were crosscorrelated and, in case of a coincidence, the values of the source with the higher likelihood value have been selected for further use. This procedure led to 45 sources in the new pointing and 22 in the old one. For each pointing separately, the X-ray sources were then crosscorrelated with the entries of the HST Guide Star Catalog (Lasker et al. 1990), to determine and correct for the systematic offset (the so-called boresight correction) between the ROSAT X-ray coordinates and the J2000 coordinate system.

The two pointings are not coaligned, but are overlapping. Thus, a lenticular region has been exposed in both observations. After having applied the boresight corrections to the single photons in the two observations, a merging was made and a new detection was performed on the lenticular region of overlap, with the same procedure described above. 26 sources have been detected in this way.

The three lists of X-ray sources (old, new and merged) were then crosscorrelated to produce the final catalog, which contains 59 sources. When a source appeared in more than one list, the detection with the highest maximum likelihood value has been selected. Positions and countrates of the sources can be found in Table 1. Notice that the countrates in Table 1 are, like the positions, those of the best detection. Variability of the sources is discussed below.

It is interesting to compare the sources detected in the old pointing with the catalog in BVS. Although the data are the same, differences arise by a better estimate of the background map, crucial for the detection procedure. Two BVS sources, X 5 and X 20, have not been confirmed by our new analysis, and 4 additional sources are detected. Thanks to the improved statistics obtained with the new observation two sources are now resolved into two separate sources each: X 11 of BVS into X 11 and X 23, X 15 of BVS into X 15 and X 24.

Most of the sources are detected with more photons at energies above than below 0.5 keV, but the number of photons is too small to make more accurate statements about the hardness ratios.

To estimate the luminosity of most sources we use a model characteristic for chromospheric emission in close binaries, similar to the models used by Dempsey et al. (1993). Specifically we use two components with temperatures of 0.175 keV and 1.4 keV, and assume that the emission measure of the hot gas is six times higher than that of the cool gas. For this model with an absorption by a column $N_{\rm H} = 1.7 \times 10^{20} {\rm cm}^{-2}$, 1 ct/ksec in the hard band corresponds to an unabsorbed flux $1.8 \times 10^{-14} {\rm erg\,cm^{-2}\,s^{-1}}$ in the 0.1-2.4 keV band, or a luminosity of $1.6 \times 10^{30} {\rm erg\,s^{-1}}$ at the distance of M 67.

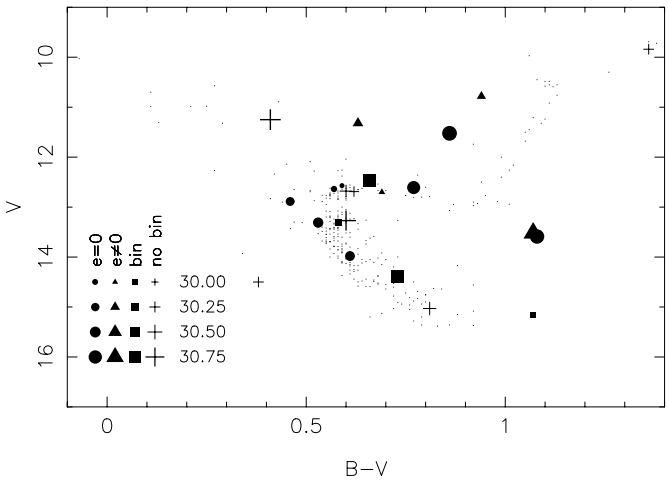

Fig. 1. Hertzsprung-Russell diagram of M 67 in which the stars detected in X-rays are indicated with special symbols. The size of a symbol is proportional to the logarithm of the X-ray luminosity in the 0.1-2.4 keV band in erg/s. The shape of a symbol indicates its spectroscopic binary status. Filled circles and triangles indicate circular binaries and eccentric binaries (i.e. eccentricity larger than 3-σ), respectively, squares indicate binaries with unknown period, and crosses indicate objects for which there is no indication of binarity. Note that for the binaries we show the total magnitude and colour.

2.1.2. Optical identifications

The optical identification of the sources in M 67 was done in several steps. We consider the two soft X-ray sources as having been identified convincingly, because their proposed optical counterparts explain their soft X-ray spectra: X 16 with the cataclysmic variable (see also Fig. 2 below), and X 23 with a white dwarf (Pasquini et al. 1994).

We searched for further identifications in three lists: binaries in M 67 with known periods; member stars according to Girard et al. (1989); and all objects listed by Montgomery et al. (1993). These lists are extensive and hence raise the issue of chance coincidences. The probability of chance coincidence depends on location in the cluster due to the radial variation of the stellar surface density. Thus for each list we have considered separately an inner area with projected distances to the cluster center $r < 8'$ and an outer area with projected distances in the range $8' < r < 18'$. The inner area corresponds to two core radii and contains roughly 50% of the cluster members (Mathieu 1983, Mathieu & Latham 1986). The outer boundary is chosen so as to contain all detected X-ray sources in the analysed area of the second ROSAT observation.

To compile the binary list we add to the list of binaries from Latham et al. (1992) the blue stragglers from Latham & Milone (1996), three contact binaries from Gilliland et al. (1991), and one orbit (for S 1113) newly determined by Mathieu et al. (1998, in preparation). We do not include the already identified cataclysmic variable in this part of our analysis. We obtain 11 identifications in the inner area, and 1 in the outer area, with binaries within the 90% error radius of an X-ray detection. We estimate the probability for chance coincidences as follows. The

Table 1. Summary of PSPC detections in the field of M 67. For each source we give the position, the 90% confidence radius, the countrate with the channel band in which it is determined (T=11-240, S=11-40, H=41-240), and where applicable the proposed optical counterparts: star numbers according to Sanders (1977) and Montgomery et al. (1993), the V magnitude, B-V color and the membership probability (mostly after Girard et al. 1989), and comments. Under comments we also indicate from which list the optical counterpart was found: L1 for binaries with known orbital period, L2 for other members of M 67, and L3 for remaining optical objects (for details and corresponding chance coincidence probabilities see Sect. 2.1.2). Information from Pasquini & Belloni (1998) is marked PB (identification or presence of Ca H&K emission or H_α emission). For sources 1-22 the sequence number is the same as in BVS; sources 5 and 20 from BVS are not found in our new analysis, and have been discarded. Source 11 from BVS is split in two sources, nos. 11 and 23; Source 15 from BVS is split in nos. 15 and 24. The other sources are newly found. Ordering of sources 1-22 and 25-61 is on declination.

X	α(2000)	δ(2000)	Δr	cts/ksec	S#	MMJ#	V	B-V	Mem.	Comment
1	8h49m53.8s	12°01′29″	16″	1.7± 0.5 H						
2	8h50m14.1s	12°01′05″	19″	1.1± 0.4 H						
3	8h49m23.4s	11°54′47″	15″	4.8± 0.8 H	262				0	L3 B=16.3
4	8h51m20.8s	11°53′26″	6″	4.6± 0.6 H	1082	6493	11.25	0.41	99	L2 PB: $H_\alpha$em.
6	8h49m54.4s	11°53′13″	9″	5.2± 0.8 T						PB: QSO
7	8h51m07.5s	11°53′01″	6″	4.4± 0.5 H	1077	5451	12.47	0.66	99	L2 PB: Ca em.; also S2224
8	8h51m13.4s	11°51′39″	5″	4.7± 0.6 H	1063	5542	13.52	1.07	99	L1 PB: Ca em.
9	8h49m35.4s	11°50′27″	16″	4.0± 0.7 H						PB: QSO(?)
10	8h51m23.7s	11°49′49″	5″	5.0± 0.6 H	1040	6488	11.52	0.88	100	L1 PB: Ca em.
11	8h51m23.1s	11°48′26″	6″	4.0± 0.5 H	1019	5748	14.38	0.73	99	L2 BVS-11a, see X 23 PB: Ca em.
12	8h50m38.5s	11°47′10″	10″	2.3± 0.5 H						
13	8h51m18.7s	11°47′00″	6″	3.4± 0.5 H	999	5643	12.60	0.78	100	L1 PB: Ca em.
14	8h51m04.2s	11°46′19″	10″	3.3± 0.5 H	759	5392	16.17	0.75	0	L3 PB: Ca em(?)
15	8h50m57.1s	11°45′52″	12″	3.2± 0.5 H						BVS-15, see X 24
16	8h51m27.1s	11°46′57″	9″	5.2± 0.7 S						CV
17	8h51m18.1s	11°44′36″	14″	0.8± 0.3 H	972	5615	15.17	1.07	42	L3 PB: Ca em.
18	8h49m42.7s	11°41′54″	21″	1.1± 0.4 H						
19	8h49m57.8s	11°41′41″	15″	1.1± 0.4 H	364				82	L3 B=11.22 PB: no Ca em.
21	8h50m11.2s	11°35′35″	14″	1.8± 0.5 H						
22	8h49m57.2s	11°34′53″	4″	85.2± 3.1 T						
23	8h51m20.6s	11°48′43″	12″	6.4± 0.8 S						BVS-11b, WD
24	8h50m56.3s	11°45′25″	12″	1.5± 0.3 H		5295	16.28	1.13		L3 BVS-15
25	8h51m27.7s	12°07′31″	15″	4.4± 0.7 T			7.77	0.5	0	L3 HD 75638 (F0)
26	8h51m25.4s	12°02′57″	8″	4.7± 0.6 H	1113	5808	13.59	1.08	94	L1 PB: Ca em.
27	8h51m43.1s	12°02′32″	12″	2.0± 0.4 H						
28	8h51m23.6s	12°01′33″	16″	1.6± 0.4 H	1112	5780	15.03	0.81	86	L2
29	8h52m22.3s	11°59′58″	16″	4.1± 0.6 H						
30	8h51m57.7s	11°59′11″	19″	5.5± 0.7 H		6289	18.84	1.24		L3
31	8h51m37.2s	11°59′03″	6″	11.7± 1.0 T	1327	6507	10.93	0.85	0	L3
32	8h51m27.3s	11°55′34″	11″	1.2± 0.3 H						S 1092 in 95% box
33	8h52m09.9s	11°55′27″	10″	4.1± 0.6 H		6401	17.36	1.63		L3
34	8h51m04.9s	11°55′24″	10″	1.1± 0.3 H		5418	20.18	1.43		L3
35	8h50m37.3s	11°54′11″	16″	1.1± 0.3 H	628	5074	14.50	0.38	69	L3
36	8h50m57.5s	11°52′48″	15″	0.5± 0.2 H						
37	8h51m22.2s	11°52′43″	9″	1.3± 0.3 H	1072	6491	11.32	0.63	99	L1
38	8h51m20.7s	11°52′10″	18″	1.6± 0.5 H	1070	5671	13.98	0.61	99	L1
39	8h50m59.1s	11°51′39″	13″	0.5± 0.2 H		5333	20.30	0.24		L3
40	8h51m37.8s	11°50′53″	8″	1.8± 0.4 H	1282	6027	13.34	0.80	99	L1 AH Cnc
41	8h51m19.0s	11°50′08″	14″	0.5± 0.2 H	1045	5654	12.55	0.59	100	L1 also S2217 (V=15.7)
42	8h51m08.1s	11°49′54″	5″	6.0± 0.6 H	1042	5457	15.79	0.88	0	L3
43	8h51m49.0s	11°49′45″	17″	1.5± 0.4 H	1270	6166	12.68	0.59	99	L2
44	8h51m02.0s	11°49′28″	13″	1.0± 0.3 H	775	5371	12.62	0.63	99	L2 also S 2214 (non-member)
45	8h51m27.9s	11°49′20″	12″	1.3± 0.3 H	1036	5833	12.80	0.50	100	L1 EV Cnc
46	8h51m24.3s	11°48′54″	19″	1.6± 0.4 S	1027	5781	13.27	0.60	100	L2 S1024 in 95% box
47	8h52m16.7s	11°48′27″	10″	2.5± 0.4 H	1601		14.57	1.02	39	L3
48	8h51m35.6s	11°48′11″	10″	1.9± 0.4 H						
49	8h50m52.2s	11°47′42″	17″	0.9± 0.3 H	760	5263	13.38	0.51	99	L2
50	8h51m35.9s	11°46′35″	11″	0.7± 0.2 H	1242	5993	12.70	0.72	99	L1

Table 1. (continued)

X	α(2000)	δ(2000)	Δr	cts/ksec	S#	MMJ#	V	B-V	Mem.	Comment
51	8h52m14.3s	$11^\circ46'25''$	$12''$	2.2± 0.4 H		6441	15.81	0.97		L3
52	8h51m50.4s	$11^\circ46'07''$	$12''$	1.0± 0.3 H	1237	6498	10.78	0.94	99	L1
53	8h51m30.5s	$11^\circ45'48''$	$17''$	0.7± 0.2 H	1234	5896	12.66	0.59	99	L1 also M5885 and M5897
54	8h51m04.8s	$11^\circ41'58''$	$11''$	1.2± 0.3 H						
55	8h52m07.0s	$11^\circ41'04''$	$15''$	0.9± 0.3 H						
56	8h52m17.4s	$11^\circ41'02''$	$17''$	1.2± 0.3 H		6468	16.90	1.68		L3
57	8h50m44.8s	$11^\circ37'50''$	$19''$	1.0± 0.3 H	727	5158	12.08	0.84	5	L3 also M5162
58	8h52m06.1s	$11^\circ37'15''$	$19''$	1.9± 0.4 H	1414	6363	14.65	0.69	26	L3
59	8h51m52.8s	$11^\circ36'01''$	$23''$	2.7± 0.5 H						
60	8h51m32.1s	$11^\circ34'03''$	$18''$	3.2± 0.6 H	924				0	L3 B=15.30
61	8h51m17.4s	$11^\circ31'54''$	$12''$	3.6± 0.6 H						

average error radius of an X-ray source is $0.2'$; with 36 binaries in the inner area, the probability that one arbitrarily chosen position is within this distance of a binary therefore is about $36 \times (0.2'/8')^2 \simeq 0.02$. The 26 X-ray sources in the inner area correspond to 26 trials, and thus the probability for 0, 1, or 2 chance coincidences are about 55%, 33%, and 10%, respectively. A similar reasoning for the outer area, which contains 6 of the binaries and 22 of the X-ray sources, shows that the probability that the one identification there is due to chance is 0.4%. We conclude that all 12 suggested identifications of X-ray sources with member binaries may well be correct; but that it is also possible that one or two identifications are spurious.

In the next step we extract from the Open Cluster DataBase of Mermilliod (1996) all stars in M 67 that have a membership probability higher than 80% according to Girard et al. (1989), and that are not included in the above-used list of binaries. This leaves 163 stars in the inner area and 148 in the outer area. For the remaining 15 X-ray sources in the inner area we obtain 7 new proposed counterparts; and for the remaining 21 X-ray sources in the outer area 3 new proposed counterparts. The probability of getting 0, 1 or 2 chance coincidences are 20%, 34% and 27%, respectively, in the inner area; and 14%, 29% and 28% in the outer area. Thus at least half of the counterparts found from probable members of M 67 in Girard et al.'s (1989) list are probably real. Similar probabilities are indicated by the occurrence of multiple possible identifications for some sources, such as X 7 and X 44. In these cases we suggest the brighter optical object as the more probable counterpart.

In the final step we compare X-ray positions with the stars in the Tables by Montgomery et al. (1993). This adds a dozen other proposed optical counterparts for the X-ray sources, almost all of them at faint magnitudes $V \gtrsim 14$; most of these may well be chance coincidences.

All suggested optical identifications can be found in Table 1. Many sources have no optical counterpart; clearly, considerable optical follow-up is needed to obtain a firm knowledge of the nature of all the X-ray sources reported in Table 1.

In the ROSAT Deep Survey, an area with $18.5'$ radius contains about 30 sources at fluxes higher than our approximate detection limit, $f(0.5-2.5\mathrm{keV}) \gtrsim 10^{-14}\mathrm{erg\,cm^{-2}\,s^{-1}}$ (see Table 4 of Hasinger et al. 1998). On the basis of this number we expect 6 background sources in our inner area, and 24 in our outer area, in the hard band (labelled H in Table 1). Of the 26 hard X-ray sources in the inner area, we identify 11 with binaries, and 7 with other M 67 members, a few of which may be due to chance. In the outer area, we identify 4 of 22 hard X-ray sources with M 67 members. The numbers of remaining unidentified sources are compatible with the estimated number of unrelated background sources.

Pasquini & Belloni (1998) have obtained high- and low-resolution spectroscopy of a number of possible optical counterparts to X-ray sources in M 67. They have identified one, possibly two X-ray sources with with QSO's (X 6 and X 9), and strengthened a number of our proposed identifications by detecting Ca H&K and/or H_α emission. This information is also indicated in Table 1.

2.2. NGC 188

NGC 188 was observed with the ROSAT PSPC on March 10-12 1993 for a total exposure time of 17597 seconds. The same procedure as described for M 67 was adopted to reduce the data, with the obvious difference that only one pointing was available. The final catalog with 34 sources is given in Table 2.

The two-component model for chromospheric emission discussed above is also applied to the sources in NGC 188. With absorption by a column $N_\mathrm{H} = 5.0 \times 10^{20}\mathrm{cm^{-2}}$, 1 ct/ksec in the hard band corresponds to an unabsorbed flux of $2.1 \times 10^{-14}\mathrm{erg\,cm^{-2}\,s^{-1}}$ in the 0.1-2.4 keV band, or a luminosity of $9.3 \times 10^{30}\mathrm{erg\,s^{-1}}$ at the distance of NGC 188.

The catalog from the membership study by Dinescu et al. (1996) has been used for the identifications of the X-ray sources in NGC 188. The criterion for identification is the same as for M 67. Suggested optical identifications are listed in Table 2.

3. Results

3.1. M 67

Parameters of detected members of M 67 are given in Table 3. The optical identifications show that we detect stars spread

Table 2. Summary of X-ray detections in NGC 188. The first five columns are the same as in Table 1. For some systems we add star ID according to Dinescu et al. (1996) and Sandage (1962), V magnitude, B-V, membership (Dinescu et al. 1996) and comments.

X	α(2000)	δ(2000)	Δr	cts/ksec	B
1	0h47m46.6s	85° 35′13″	11″	2.0± 0.4	H
2	0h36m48.1s	85° 35′09″	19″	8.9± 0.9	H
3	0h38m20.1s	85° 34′27″	23″	2.0± 0.5	T
4	0h36m46.4s	85° 32′23″	14″	1.7± 0.4	H
5	0h44m50.0s	85° 32′01″	12″	1.1± 0.3	H
6	0h39m12.4s	85° 31′26″	4″	37.4± 1.6	T
7	0h42m34.5s	85° 31′21″	14″	0.9± 0.3	H
8	0h46m21.9s	85° 30′53″	12″	8.4± 0.8	H
9	0h37m32.6s	85° 30′14″	16″	1.1± 0.3	H
10	0h42m43.5s	85° 29′07″	15″	1.3± 0.3	H
11	0h36m37.3s	85° 28′59″	15″	1.1± 0.3	H
12	0h37m55.9s	85° 28′46″	10″	1.9± 0.4	H
13	0h44m35.2s	85° 27′07″	12″	0.8± 0.2	H
14	0h39m43.5s	85° 26′38″	13″	0.9± 0.3	H
15	0h33m01.0s	85° 24′52″	4″	40.0± 1.6	H
16	0h51m30.7s	85° 24′46″	13″	1.0± 0.3	H
17	0h45m22.0s	85° 23′40″	15″	0.8± 0.3	H
18	0h37m54.6s	85° 22′54″	11″	1.1± 0.3	H
19	0h50m26.3s	85° 22′06″	5″	7.6± 0.7	H
20	0h47m42.4s	85° 22′04″	9″	1.3± 0.3	H
21	0h49m58.9s	85° 21′14″	12″	0.6± 0.2	H
22	0h54m16.6s	85° 20′27″	10″	2.4± 0.4	H
23	0h34m18.3s	85° 19′20″	21″	2.4± 0.5	H
24	0h32m29.4s	85° 18′42″	12″	2.2± 0.4	H
25	0h42m59.1s	85° 18′20″	15″	0.6± 0.2	H
26	0h51m22.1s	85° 17′57″	4″	19.7± 1.1	H
27	0h45m27.7s	85° 16′36″	5″	5.0± 0.6	H
28	0h33m02.0s	85° 16′22″	6″	11.4± 0.9	H
29	0h47m54.3s	85° 14′55″	8″	1.8± 0.3	H
30	0h42m42.7s	85° 14′15″	5″	9.7± 0.8	H
31	0h39m08.0s	85° 12′41″	12″	1.2± 0.3	H
32	0h41m27.1s	85° 12′30″	13″	0.9± 0.3	H
33	0h43m53.8s	85° 06′25″	11″	3.9± 0.5	H
34	0h37m30.3s	85° 05′34″	7″	10.1± 0.8	H

Suggested identifications; comments

X	D#	S#	V	B-V	Mem.	Comment
1	1824		14.56	0.83	<60	
2						Extended?
5	1819		13.98	1.20	<60	
6	1861		14.91	1.58	<60	
8						Extended?
11	1855		12.74	0.49	<60	
21	1335	III-108	15.58	0.72	95	
26	1361	III-89	13.16	0.81	1?	V8
29	719	I-1	11.76	1.18	100	FK Com
31					D799 in 95% box	

throughout the Hertzsprung-Russell diagram of M 67, as shown in Fig. 1. Accordingly, the types of the detected systems are varied. Many are known photometric or spectroscopic binaries, including a cataclysmic variable (X 16), two contact binaries (X 40 and X 45), three (probable) RS CVn type systems (X 13, X 38 and X 41), a circular binary consisting of a giant and a white dwarf (X 10), a circular binary in a triple system (X 53), three eccentric binaries (X 37, X 50 and X 52), two binaries located below the subgiant branch (X 8 and X 26), and a few spectroscopic binaries for which there are not yet orbit solutions. In addition we detect several sources for which there is no indication of binarity, including a blue straggler (X 4). The orbital periods of the binaries in M 67 detected in X-rays range from 0.36 d to 1495 d. The detection of binaries with eccentric orbits, and of some binaries with orbital periods $P_b \gtrsim 40$ d is rather surprising as no tidal interaction is thought to take place in these (Verbunt & Phinney 1995).

With the exception of the two contact binaries and of the cataclysmic variable, all binaries referred to below are spectroscopic binaries. Many of them are discussed in some detail in Mathieu et al. (1990). We now proceed to discuss the sources according to category.

Table 3. Summary of detected members (probability >40%) in M 67. For each X-ray source we give the Sanders number, the X-ray luminosity in $0.1 - 2.4$ keV band, orbital period, orbital eccentricity, and the binary type. All X-ray luminosities assume an X-ray spectrum typical for chromospheric emission. This does not apply to the white dwarf and the cataclysmic variable. SB indicates a spectroscopic binary from the survey of Latham and Mathieu without a determined orbit solution.

X	S#	$L_{\rm X}$(erg/s)	$P_{\rm b}$(d)	e	type
4	1082	7.2×10^{30}			blue straggler
7	1077	6.8×10^{30}	SB		RS CVn?
8	1063	7.3×10^{30}	18.39	0.22	sub-subgiant
10	1040	7.8×10^{30}	42.83	0.00	giant+white dwarf
11	1019	6.2×10^{30}	SB		RS CVn?
13	999	5.3×10^{30}	10.06	0.00	RSCVn
16	–		0.09	0.00	catacl. var.
17	972	1.2×10^{30}	SB		RS CVn?
19	364	1.7×10^{30}			
23	–				white dwarf
26	1113	7.3×10^{30}	2.82	0.03	sub-subgiant
28	1112	2.5×10^{30}			RS CVn??
35	628	1.7×10^{30}			catacl. var.??
37	1072	2.0×10^{30}	1495.	0.32	
38	1070	2.5×10^{30}	2.66	0.00	RS CVn
40	1282	2.8×10^{30}	0.36	0.00	W Uma
41	1045	0.8×10^{30}	7.65	0.00	RS CVn
43	1270	2.3×10^{30}			
44	775	1.6×10^{30}			
45	1036	2.0×10^{30}	0.44	0.00	W Uma
46	1027	6.5×10^{30}			
49	760	1.4×10^{30}	SB		RS CVn?
50	1242	1.1×10^{30}	31.78	0.66	
52	1237	1.6×10^{30}	697.8	0.11	
53	1234	1.1×10^{30}	4.36	0.06	triple system

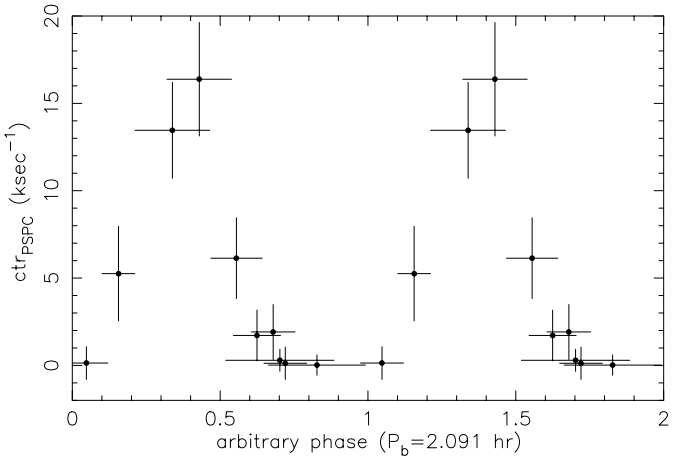

Fig. 2. The folded X-ray lightcurve of EU Cnc. The 100% variation is characteristic for AM-Her type systems.

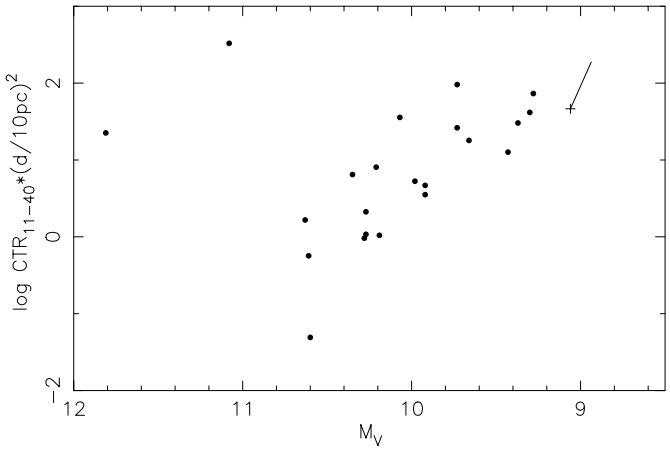

Fig. 3. X-ray countrates of white dwarfs detected in the ROSAT All Sky Survey (from Fleming et al. 1996), normalized to a distance of 10 pc, as a function of absolute magnitude. The observed countrate for the white dwarf in M 67 is indicated by $+$; the correction for interstellar absorption depends strongly on the spectrum: the line indicates the correction for an assumed 35 eV black body X-ray spectrum.

3.1.1. The cataclysmic variable EU Cnc

Source X 16 is the cataclysmic variable EU Cancri. This variable was discovered by Gilliland et al. (1991) at a photometric period of 2.09 hr. It is of the AM-Her type, i.e. a binary in which a white dwarf with a strong magnetic field accretes from a low-mass main-sequence dwarf, and in which the rotation of the white dwarf is locked to the orbital revolution. EU Cnc is detected with ROSAT only at soft energies (channels 11-40, corresponding roughly to 0.1-0.4 keV), at a countrate $\mathrm{ctr}_{11-40} = 0.0052$ cts/s. Folding the X-ray data at the binary period, we obtain the lightcurve shown in Fig. 2. The predominance of soft photons is typical for AM-Her type systems, as is the almost 100% modulation of the X-ray lightcurve (due to occultation of the X-ray emission region by the rotating white dwarf). The ratio of ctr_{11-40} to the optical flux also is in the range observed for AM-Her type systems (see for example Table 1 of Verbunt et al. 1997). Our observations thus confirm the suggestion by Gilliand et al. (1991) that this object is an AM-Her type system.

Conversion of the observed countrate to flux suffers from our ignorance of the spectrum; for an assumed blackbody spectrum with $kT_{\mathrm{bb}} = 35 - 60$ eV we find a bolometric X-ray luminosity for EU Cnc of $L_{\mathrm{X}} = 1.2 - 0.7 \times 10^{31} \mathrm{erg\,s^{-1}}$ at the distance and column of M 67.

3.1.2. The hot white dwarf

X 23 is a very soft source, and has been identified with a white dwarf by Pasquini et al. (1994). The effective temperature of this star is $T_{\mathrm{eff}} = 68,000 \pm 3,000$ (Fleming et al. 1997), which is hot enough to explain the X-ray emission. To compare its countrate with that of nearby field white dwarfs, we take the countrates found by Fleming et al. (1996) in the ROSAT All Sky Survey, for white dwarfs whose absolute magnitudes are given in the spectroscopic studies of Bergeron et al. (1992) and Bragaglia et al. (1995). The values thus found are shown in Fig. 3; it is seen that the countrate we detect for the white dwarf in M 67 is in the range seen for field white dwarfs at comparable magnitudes.

3.1.3. Contact binaries

The two contact binaries detected in M 67 are AH Cnc (X 40, S 1282) and EV Cnc (X 45, S 1036, no. III-2 of Gilliland et al. 1991). The countrates are at the limit of detection. Contact binaries are thought to be X-ray emitters due to chromospheric activity, induced by the rapid rotation of the stars comprising the binary. The X-ray luminosities of these two contact binaries may be compared with those of contact binaries in the field, studied by McGale et al. (1996). The countrates of AH Cnc and EV Cnc are between those of e.g. V389 Oph and AK Her, converted to the distance of M 67. EV Cnc has an orbital period slightly longer than that of AK Her, which has the longest orbital period of the systems discussed by McGale et al. A third contact binary in M 67, ET Cnc (=III-79), was not detected; it is much fainter in the optical than the other two, at $M_V \simeq 16$.

3.1.4. RS CVn systems

We detect three circular binaries at orbital periods $P_b \lesssim 10$ d. The circularity of the orbits indicates strong tidal interaction, and we expect that these systems are chromospherically active binaries; optical spectroscopy is required to confirm this. S 999 and S 1045 are double-lined spectroscopic binaries discussed by Mathieu et al. (1990). S 999 = X 13 is a binary of a slightly evolved star, hence mass equal to the turnoff mass $1.25\,M_\odot$ of M 67, and a $1.09\,M_\odot$ main sequence companion. S 1045 = X 41 is a binary of two main sequence stars of equal masses $1.18\,M_\odot$. S 1070 = X 38 lies on the main-sequence in the Hertzsprung Russell diagram of M 67; its orbital period $P_b = 2.66$ d and circular orbit suggest that it is an RS CVn binary. The larger star

in RS CVn binaries is forced by the tidal interaction to corotate with the orbit, and this rapid rotation enhances the chromospheric activity, which explains the X-ray emission. The X-ray luminosities of the RS CVn systems in M 67 is compared with those of RS CVn systems in the field in Fig. 4. For the conversion of observed countrate to X-ray luminosity we use the two-temperature model described in Sect. 2.1.1. It is seen that the X-ray luminosities of the M 67 systems are comparable to those of RS CVn systems in similar locations of the Hertzsprung Russell diagram.

X 53 is identified with S 1234. Mathieu et al. (1990) observe that S 1234 is a triple system in which the primary and tertiary have roughly equal light. The period of 4.36 d is then the orbital period of the inner binary. The visible stars would have masses close to $1.18\,M_\odot$; no strong constraints exist for the mass of the companion in the inner binary. The X-ray emission of S 1234 is probably due to chromospheric activity in the inner binary: the inner orbital period is short enough for tidal interaction to be efficient.

Four binaries with as yet unknown orbital solutions have also been detected in X-rays (X 49 = S 760, X 17 = S 972, X 11 = S 1019, X 7 = S 1077). All but S 760 appear to have orbital periods of $\leq$ 10 days (for S 1077 see Mathieu et al. 1990), suggesting that they too are RS CVn systems.

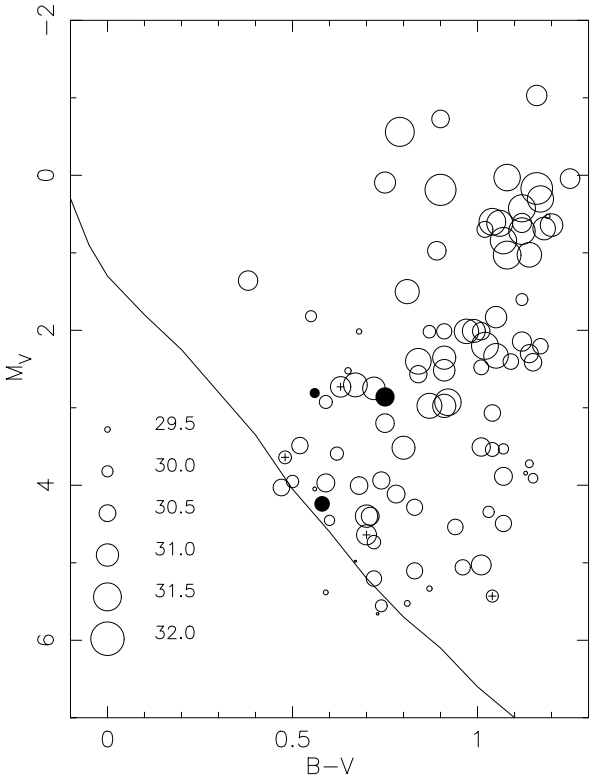

Fig. 4. X-ray luminosities of RS CVn systems detected in the ROSAT All Sky Survey (open circles; data from Dempsey et al. 1993) and detected in M 67 (filled circles), as a function of their location in the Hertzprung Russell diagram. Colours and magnitudes are for the total light of the binary. The size of the symbols is proportional to the logarithm of the X-ray luminosity (in erg/s). The solid line indicates the main sequence. Four binaries in M 67 with unknown binary parameters presumably also are RS CVn systems, and are also shown (circles with inscribed +). Corrections for interstellar absorption have been made for the M 67 systems only; the corrections for the field systems are expected to be small. The X-ray luminosities for the RS CVn systems in M 67 are similar to those of the field systems.

3.1.5. S 1040

X 10 is identified with S 1040. S 1040 was discovered to be a circular binary by Mathieu et al. (1990). Verbunt & Phinney (1995) showed that the giant in this binary is too small to be responsible for the orbital circularization, and concluded that the companion to the giant must be a white dwarf, whose progenitor filled its Roche lobe as a giant and circularized the orbit. The companion to the giant has been detected in the ultraviolet, and its ultraviolet spectrum shows that it is indeed a white dwarf, with a temperature $T_{\rm eff} = 16,160$ K (Landsman et al. 1997).

The white dwarf is too cool to be responsible for the X-ray luminosity, which therefore is presumably due to chromospheric activity of the giant (Belloni et al. 1993). Such activity is evident from the Mg II λ 2800 doublet which is in emission (Landsman et al. 1997), and also from Ca H&K emission (Pasquini & Belloni 1998). We suggest that this chromospheric activity may be a remaining effect of the phase of mass transfer in the earlier evolution of this binary.

3.1.6. Stars below the subgiant branch

X 8 and X 26 are identified with S 1063 and S 1113 respectively. This means that both stars located below the subgiant branch in the Hertzsprung Russell diagram of M 67 have now been detected in X-rays. S 1063 is an eccentric binary with an orbital period of 18.3 d; S 1113 is a circular binary with a period of 2.82 d (Latham et al. 1992; Mathieu et al. 1998, in preparation). The nature of these stars, why they are located below the subgiant branch, and why they emit X-rays, is a mystery. This is all the more remarkable, as these two stars belong to the brightest X-ray sources in M 67. Model computations show that the larger star in S 1063 could be synchronized with the orbital motion at periastron (Van den Berg et al. 1998, in preparation). For $e = 0.22$ this corresponds to a rotation period which is 60% of the orbital period.

The X-ray emission of S 1063 (X 8) is variable: the countrate in November 1991 was 8.1 ± 0.9/ksec, that in April 1993 4.7 ± 0.6/ksec.

3.1.7. Other eccentric binaries

X 50 has been identified with S 1242, an eccentric binary with an orbital period of almost 32 d. X 37 and X 52 have been identified with S 1072 and S 1237, respectively, two long-period eccentric binaries, whose positions in the Hertzsprung Russell diagram could suggest that they contain evolved stars (Figs. 1). The colour and magnitude of S 1237 can be produced by the combination of a giant branch star and a main-sequence star

close to the turnoff (Janes & Smith 1984). No satisfactory solution has been suggested yet to explain the magnitude and colour of S 1072 (see e.g. Mathieu et al. 1990).

It is not clear to us why these three eccentric binaries emit X-rays. We don't think that the X-ray emission is due to hot white-dwarf companions, because the X-ray spectrum is not as soft as would be expected for a white dwarf. Also, the progenitor of the white dwarf would likely have circularized the orbit in its giant stage: even an orbit of several thousand days can be circularized by a white dwarf progenitor, as witnessed by S 1221 (Verbunt & Phinney 1995).

3.1.8. No indication of binarity

A number of X-ray sources can be identified with stars for which there is no indication that they are binaries. It cannot be excluded that these stars are chance coincidences. X 43 = S 1270 and X 44 = S 775 have been observed by Latham & Mathieu; no radial velocity variation was found, so these stars are not close binaries. X 28 = S 1112 has not been measured by Latham & Mathieu. X 35 is S 628, located to the left of the main-sequence; such a location can arise when a main-sequence star is accompanied by a hot white dwarf. The hardness of the X-ray spectrum argues against a hot non-accreting white dwarf. Perhaps S 628 is a cataclysmic variable. It should be noted that its membership probability is only 69%; if it is at larger distance than M 67 (to be at or above the main sequence it has to be $\gtrsim 2.5$ times the distance of M 67), its X-ray luminosity is accordingly higher.

X 4 is the blue straggler S 1082. This has been suggested to be in a binary with a sdO companion on the basis of a large ultraviolet excess with respect to the spectrum derived from Strömgren photometry (Landsman et al. 1998). A binary period of approximately 1 day has been suggested from optical photometry (Goranskij et al. 1992). However, the large velocity variations implied by such a short period have not been found by Mathieu et al. (1986), even though they note that the dispersion in their velocities for this star is somewhat larger than normal. The larger dispersion may be due to the early spectral type. X 19 is S 364, close to the location of the Mira variables in the Hertzsprung Russell diagram. No chromospheric emission is present in S 364 (Pasquini & Belloni 1998).

3.1.9. Non-members

X 25 is identified with HD 75638. This star is a triple star, with an inner orbit of 5.8 d and zero eccentricity (Nordström et al. 1997). The X-ray luminosity suggests that the inner binary is a RS CVn system.

X 42 shows a flare in the last 2800 s of our observations, during which the countrate was 0.03 cts/s, which is about ten times higher than the average countrate before. Such a flare suggests that S 1042 may be a late main-sequence star; its colour and magnitude are compatible with a K dwarf at the distance of M 67. However, according to Girard et al. (1989) S 1042 is not a member.

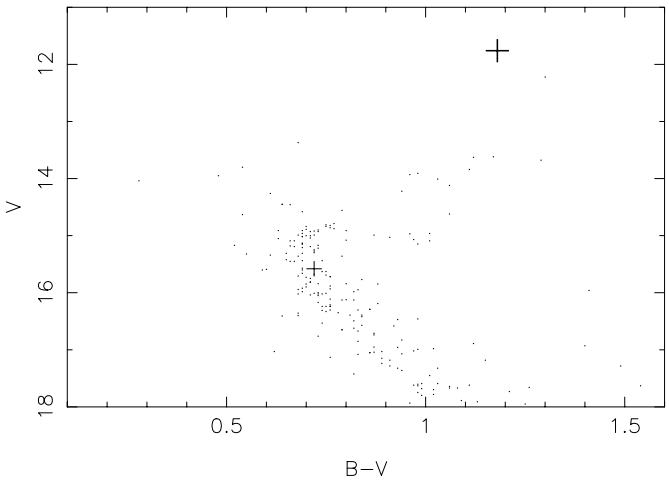

Fig. 5. Hertzsprung Russell diagram of NGC 188 (data mainly from Caputo et al. 1990) showing as + the two detected X-ray sources.

3.2. NGC 188 and V 8

In Fig. 5 we show the Hertzsprung Russell diagram of NGC 188 with the two detected member stars, X 29 and X 21. X 29 = D 719 is one of the brightest giants in NGC 188, and remarkable because of its relatively rapid rotation, at $v \sin i \simeq 24$ km/s and Ca H and K emission. The absence of radial-velocity variations suggest that it is a single, rapidly rotating giant, an FK Comae-type star (Harris & McClure 1985). The X-ray luminosity of the star, $L_{0.1-2.4\mathrm{keV}} = 1.7 \times 10^{31} \mathrm{erg\,s^{-1}}$, is in agreement with this suggestion.

High-precision radial-velocity measurements obtained with the WIYN telescope show X 21 = D 1335 to be both a short-period velocity variable and a rapid rotator (Mathieu & Dolan 1998, in preparation). Thus the X-ray emission at $L_{0.1-2.4\mathrm{keV}} = 5.6 \times 10^{30} \mathrm{erg\,s^{-1}}$ is likely due to chromospheric activity. The star has been investigated for photometric variability by Kaluzny & Shara (1987), who do not find it variable.

X 26 = D 1361 is variable V 8 of Kaluzny & Shara (1987), who find evidence for a 2.66 day periodicity in the B magnitude, and suggest that the star is of the FK Comae type. The proper motion of this star suggests that it is not a member of NGC 188 (Dinescu et al. 1996). If it is a member, its X-ray luminosity is 1.8×10^{32} erg/s.

4. Conclusions

The increased sensitivity of the X-ray observation of M 67 and the improved optical information have led to a true plethora of source types, as illustrated by Table 3. Many of these are more or less expected source types, such as the cataclysmic variable, the hot white dwarf, the contact binaries, and the circular short-period binaries: for all of these the X-ray luminosity is in the range found for similar sources in the galactic disk. Interestingly however, several sources have been detected for which we do not understand the mechanism of X-ray emission. These include several binaries with eccentric orbits, of which two are located in the Hertzsprung Russell diagram below the subgiant branch.

Unexpected also are the detection of a binary of a giant and a white dwarf in a circular orbit; and of a blue straggler that appears to be a single star.

Further optical studies of these objects may help in elucidating the mechanism(s) of X-ray emission. For example, chromospheric activity can be detected in the form of H α or Ca H and K emission; and is probably caused by rapid rotation which may be detected through line broadening. If mass transfer is taking place in any of these binaries, broad Balmer emission lines are expected.

The number of X-ray sources detected in NGC 188 is much lower, due to the higher detection flux limit. One of the two detected members is a single, rapidly rotating giant star, an FK Com type object - which adds yet another source type. We predict that a more sensitive X-ray observation of NGC 188 will detect a few dozen X-ray sources, similar to those we have found in M 67.

Acknowledgements. This work builds on the Center for Astrophysics M 67 binary survey, for which we express our appreciation to Dr. David Latham. RDM was supported by a National Science Foundation grant AST-9731302. In identifying our X-ray sources we have made use of the Open Cluster DataBase of Mermilliod (1996).

References

Belloni T., Tagliaferri G. 1997, A&A, 326, 608
Belloni T., Verbunt F. 1996, A&A, 305, 806
Belloni T., Verbunt F., Schmitt J. 1993, A&A, 269, 175
Bergeron P., Saffer R., Liebert J. 1992, ApJ, 394, 228
Bragaglia A., Renzini A., Bergeron P. 1995, ApJ, 443, 735
Caillault J.-P. 1996, in H. Zimmermann, J. Trümper, H. Yorke (eds.), Roentgenstrahlung from the Universe, MPE Report 263, p. 1
Caputo F., Castellani V., Chieffi A., Collados M. C. M. R., Paez E. 1990, AJ, 99, 261
Cruddace R., Hasinger G., Schmitt J. 1988, in F. Murtagh, A. Heck (eds.), Astronomy from large databases, p. 177
Dempsey R., Linsky J., Fleming T., Schmitt J. 1993, ApJS, 86, 599
Dinescu D., Demarque P., Guenther D., Pinsonneault M. 1995, AJ, 109, 2090
Dinescu D., Girard T., van Altena W., Yang T., Lee Y.-W. 1996, AJ, 111, 1205
Fleming T., Snowden S., Pfeffermann E., Briel U., Greiner J. 1996, A&A, 316, 147
Fleming T., Liebert J., Bergeron P., Beauchamp A. 1997, in J. Isern, M. Hernanz, E. Garcia-Berro (eds.), Tenth European Workshop on White Dwarfs, Kluwer, Dordrecht, 91
Gilliland R., Brown T., Duncan D., et al. 1991, AJ, 101, 541
Girard T., Grundy W., López C., van Altena W. 1989, AJ, 98, 227
Goranskij V., Kusakin A., Mironov A., Moshkaljov A., Pastukhova E. 1992, Astron. Astroph. Transactions, 2, 201
Harris H., McClure R. 1985, PASP, 97, 261
Hasinger G., Burg R., Giacconi R. et al. 1998, A&A, 329, 482
Janes K., Smith G. 1984, AJ, 89, 487
Kaluzny J., Shara M. 1987, ApJ, 314, 585
Landsman W., Aparicio J., Bergeron P., Di Stefano R., Stecher T. 1997, ApJ (Letters), 481, L93
Landsman W., Bohlin R., Neff S. et al. 1998, AJ, in press
Lasker B., Sturch C., McLean B. et al. 1990, AJ, 99, 2019
Latham D., Milone A. 1996, in E. Milone, J.-C. Mermilliod (eds.), The origins, evolutions, and destinies of binary stars in clusters, ASP Conference Series 90, p. 385
Latham D., Mathieu R., Milone A., Davis R. 1992, in A. Duquennoy, M. Mayor (eds.), Binaries as tracers of stellar formation, Cambridge University Press, Cambridge, p. 132
Mathieu R. 1983, *Ph.D. thesis*, University of California, Berkeley
Mathieu R., Latham D. 1986, AJ, 92, 1364
Mathieu R., Latham D., Griffin R., Gunn J. 1986, AJ, 92, 1100
Mathieu R., Latham D., Griffin R. 1990, AJ, 100, 1859
McGale P., Pye J., Hodgkin S. 1996, MNRAS, 280, 627
Mermilliod J.-C. 1996, in E. Milone, J. Mermilliod (eds.), The origin, evolution and destiny of binary stars in clusters, ASP Conference Series, ASP, San Francisco, p. 475
Montgomery K., Marschall L., Janes K. 1993, AJ, 106, 181
Nordström B., Stefanik R., Latham D., Andersen J. 1997, A&AS, 126, 21
Pasquini L., Belloni T. 1998, A&A, 336, 902
Pasquini L., Belloni T., Abbott T. 1994, A&A, 290, L17
Predehl P., Schmitt J. 1995, A&A, 293, 889
Randich S., Schmitt J., Prosser C. 1996, in H. Zimmermann, J. Trümper, H. Yorke (eds.), Roentgenstrahlung from the Universe, MPE Report 263, p. 61
Sandage A. 1962, ApJ, 135, 333
Sanders W. 1977, A&AS, 27, 89
Twarog B., Anthony-Twarog B. 1989, AJ, 97, 759
Verbunt F., Bunk W., Ritter H., Pfeffermann E. 1997, A&A, 327, 602
Verbunt F., Phinney E. 1995, A&A, 296, 709
von Hippel T., Sarajedini A. 1998, AJ, in press
Zimmermann H., Becker W., Belloni T., et al. 1994, EXSAS User's Guide: Extended scientific analysis system to evaluate data from the astronomical X-ray satellite ROSAT, Technical Report 257, MPE